Pergamon

0301-9322(95)00052-6

Int. J. Multiphase Flow Vol. 22, No. 1, pp. 121–132, 1996

0301-9322/96 $15.00 + 0.00

LARGE AND SMALL BUBBLE INTERACTION PATTERNS IN A BUBBLE COLUMN

K. TSUCHIYA†, K. OHSAKI and K. TAGUCHI

Department of Chemical Science and Technology, The University of Tokushima, Tokushima 770, Japan.

(Received 15 December 1994; in revised form 15 June 1995)

Abstract—A visual analysis is made on the fate of a large (or "cap") bubble injected into a swarm of otherwise uniformly dispersed small bubbles; experiments, covering gas holdups for the swarm bubbles as high as 6%, are conducted in a two-dimensional column to ensure the distinct appearance of a single cap throughout its rise in the swarm. Specific focus is on the stability or breakup of the large bubble induced by the overtaken small bubbles. The diversity of cap–bubble interactions is observed and classified based on the observed shape distortion and/or breakup patterns into seven modes. The probability of occurrence of each mode is estimated, the results of which indicate that there exists a critical gas holdup (e.g. ~0.01 for tap water) beyond which the degree of cap–bubble interactions sharply increases. This general trend is found for the other liquids tested (i.e. sodium sulfite and glycerin solutions) with lower degrees of interactions and the transition being less distinct. The effects of the swarm gas holdup on the specific interaction properties are also studied: with increasing holdup, the axial location of the breakup event shows a noticeable tendency of shifting from lower to higher positions; the size ratio of two daughters after the split tends to approach unity; the dominating breakup mechanism shifts from the inherent instability of the cap itself to the bubble attachment at the cap base, which triggers the ultimate necking and "pinching-off", to the acceleration of the cap toward (usually two) preceding bubbles under the influence of their wakes.

Key Words: cap–bubble interaction, shape distortion, bubble breakup, necking, pinching-off, bubble hole

INTRODUCTION

In the practical operation of industrial bubble column reactors (BCRs), the prevailing flow regime is mostly heterogeneous; the bubble flow structure is extremely complex due to the presence of a swarm of bubbles with broad distributions of rise characteristics such as bubble size, bubble rise velocity and gas holdup throughout the column. While the most rigorous analysis requires taking into account a number of (almost continuous) bubble classes of different bubble sizes and residence times, it is often modeled by a bimodal size distribution (Deckwer & Schumpe 1993). Under such simplified circumstances, the interaction between the large bubbles and the surrounding small ones plays an important role.

A few studies have focused on specific interactions between large and small bubbles. Hills (1975) appears to be the first to study the influence of a swarm of small bubbles on the rise of a large bubble, referred to as a "cap" to distinguish it from each "bubble" constituting the swarm—the same convention applies in this study. He attempted to predict the trajectories of individual bubbles overtaken by a cap in swarms of low gas holdups, thus in the absence of direct cap–bubble interactions. His important findings are: there exists a "hole" of gas holdup, or a region of negligible bubble population, right above the cap frontal surface; at high holdups (>4%), marked concentrations of bubbles appear around the hole and promote bubble coalescence, thus the formation of secondary "satellite caps," which then rise in the wake of the primary cap and coalesce with it.

Following Hills' work, most studies have directed their efforts toward examining the enhancement of the cap rise velocity in the presence of the surrounding bubbles. Hills & Darton (1976) reached a conclusion that the enhancement is not necessarily due to "gulf-stream" circulation of the liquid phase nor to bubble coalescence, but probably results from small-scale turbulent eddies in the liquid phase generated by the swarm bubbles. This latter contribution tends to distort the

†To whom correspondence should be addressed.

frontal surface of the cap thereby altering the liquid flow pattern around the bubble nose. Miyahara & Fan (1992) found, in a gas–liquid–solid fluidized bed, that the extent of enhancement of the cap velocity can be estimated by applying the concept of "wake velocity"—in essence, a contribution of the liquid circulation induced by the bubble swarm—for in-line caps (Marks 1973; Miyahara *et al.* 1991).

The present study concerns the visual observation of the fate of a large bubble injected into a swarm of otherwise uniformly dispersed small bubbles. For this purpose, experiments are conducted exclusively in a two-dimensional column to ensure the distinct appearance of a single cap throughout its rise in the swarm over a wide range of gas holdups. The specific focus is on the stability or breakup of the large bubble induced by the surrounding/overtaken small bubbles. The effect of the liquid-phase properties on the interaction characteristics is also examined.

EXPERIMENTAL

Figure 1 shows a schematic diagram of the experimental setup used in this study. The two-dimensional column is made of transparent PVC and has a main section of 1.0 m effective height, 0.218 m width and 10 mm gap thickness. Below this section is the gas-distributing section which consists of a gas plenum of five isolated, equal-sized compartments and a 5 mm thick PMMA porous plate of 30 μm pore size and 35% porosity (Spacy Chemical Inc., Tokyo) fixed separately above each compartment. The total gas flow into the column is controlled by the orifice flow meter; the gas flow through each compartment is individually regulated by a needle valve so as to attain even distribution of gas flow, i.e. a uniform swarm of small bubbles throughout the column.

A separate gas injection is made through a 4.0 mm i.d. (1.0 mm thick) stainless steel nozzle, with a tapered (to o.d.) outlet, flush-mounted on the rear wall at a distance of 181 mm above the top of the gas-distributing section. A single, large/cap bubble with no satellites can be readily generated; the bubble size is controlled roughly by altering the opening time of the solenoid valve, which is regulated by an electric pulse-signal generator, and precisely by regulating the gas delivery pressure with the digital pressure gauge of ± 10 Pa precision.

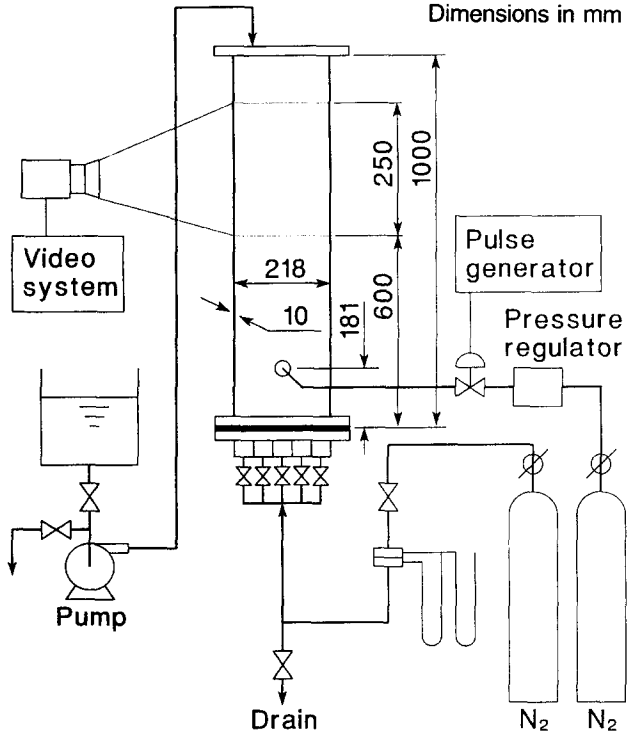

Figure 1. Schematic diagram of the experimental set-up.

Table 1. Physical properties of liquids

Liquid	Density (kg/m^3)	Viscosity (mPa s)	Surface tension (mN/m)
Tap water	998	0.96	72.5
75 mol/m^3 Na_2SO_3	1007	1.0	73.0
60 wt% Glycerin	1148	10.1	65.8

Table 2. Specific experimental conditions

Water			Sodium sulfite solution			Glycerin solution		
$10^2 U_G$ (m/s)	$10^2 \epsilon_G$ (−)	d_e† (mm)	$10^2 U_G$ (m/s)	$10^2 \epsilon_G$ (−)	d_e† (mm)	$10^2 U_G$ (m/s)	$10^2 \epsilon_G$ (−)	d_e† (mm)
0.083	0.46	2.3 ± 0.4	0.083	0.46	1.1 ± 0.2	0.118	0.35	2.0 ± 0.3
0.167	0.94	—	0.146	0.94	—	0.125	0.47	—
0.186	1.05	—	0.168	1.05	—	0.145	0.70	—
0.265	1.64	3.2 ± 0.6	0.253	1.63	1.4 ± 0.3	0.155	0.80	1.9 ± 0.1
0.373	2.31	—	0.406	2.31	—	0.168	0.92	—
0.537	3.23	—	0.515	3.23	—	0.188	1.04	—
0.654	4.00	4.0 ± 0.7	0.687	4.03	1.5 ± 0.4	0.239	1.60	1.8 ± 0.1
0.771	4.63	—	0.780	4.58	—	0.305	2.27	—
0.845	5.14	—	0.868	5.12	—	0.434	3.25	—
1.04	5.99	4.2 ± 0.7	1.02	5.98	2.0 ± 0.6	0.574	3.96	2.3 ± 0.3

†Measured for selected runs.

A video camera system is utilized to obtain: (1) the rise characteristics of each cap, including the rise velocity and the shape/dimensions [mainly the major axis (breadth) and minor axis (height)]; (2) the state of redispersion of swarm bubbles around the "disturbing" cap; and (3) the fate (i.e. shape distortion or breakup) of the cap under the influence of directly/indirectly interacting swarm bubbles. The video camera is fixed mostly at a location 0.725 m above the gas distributor so as to obtain an effective observation zone spanning a vertical distance between 0.60 and 0.85 m. The cap rise characteristics are measured by analyzing frame-by-frame the recorded video images, which are obtained over an exposure time of 1/1000 s or 1/250 s at 30 frames/s. Under each experimental condition (with at least 100 cap injections), the cap–bubble interactions are closely monitored and, as supplemental information, the average size of the bubble hole is determined.

Nitrogen is used as the gas phase for both the swarm and the cap bubbles; tap water, sodium sulfite solution or glycerin solution is used as the liquid phase (see table 1 for their physical properties). The swarm gas holdup is estimated from the measurement of the aerated and unaerated liquid levels for each superficial gas velocity (U_G) tested over the range 0–0.01 m/s. The specific experimental conditions including the gas holdup (ϵ_G) and the mean (projection-equivalent) bubble diameter (d_e, measured for limited runs) are summarized in table 2. To assure reasonable distinction between the two classes of bubbles, and at the same time to avoid any excess destabilization of the caps and excess wall effects caused by the side walls, the size of the single caps in this study is fixed at 28.4 ± 1.6 mm in breadth (b). All the experiments are conducted in the temperature range 22 ± 2°C.

RESULTS AND DISCUSSION

Modes of cap–bubble interactions

While rising through a swarm of small bubbles, a large bubble or cap was observed to exhibit a variety of shape distortion and/or breakup patterns. In the present study, seven modes of interaction patterns could be recognized; table 3 describes the specific feature of each mode. In mode I no breakage nor noticeable shape distortion particularly different from the isolated cap case is observed. Mode II signifies the deformation which can lead to eventual breakage, often characterized by indentation along the cap frontal surface. Depending on the extent/depth or location of such surface depression, the cap may or may not disintegrate (see the discussion in the following subsection). Another pattern of shape distortion is categorized separately as mode VII; in this case, contrary to the general notion of no bubble-to-cap attachment along the cap roof (refer

Table 3. Modes of breakup patterns of cap bubble

Mode	Description
I	No breakup; the same stability as an isolated single cap
II	Nearly (but not) breaking up; marked distortion (flattening) with occasional indentation
III	Breakup into two equal-sized bubbles†
IV	Breakup into two different-sized bubbles
V	Breakup immediately followed by collision (then possible coalescence)
VI	Breakup into three (or more) bubbles
VII	Cap becoming prolate (or deformed considerably at least) in the presence of a small bubble near the cap nose

†Two bubbles of breadths b_1 and b_2 ($b_1 \geqslant b_2$) are regarded as identical if $b_2/b_1 \geqslant 0.8$.

to the presence of the "hole" mentioned in the introduction; Hills 1975; Fan & Tsuchiya 1990), the cap rushes into and eventually attaches to a small bubble ahead of it. During the acceleration process, the cap alters its shape from a regular oblate cap shape to a nose-peaked, mountain-like shape to a profoundly elongated (along the direction of its movement, i.e. prolate) shape.

Modes III–VI concern the cap–bubble interactions that have ended up with cap breakage over the range of gas–liquid dispersion height examined in this study (≈ 0.8 m). The cap may split into two daughter bubbles, the sizes of which are almost identical ($0.8 \leqslant b_2/b_1 \leqslant 1$ with b_1 being the breadth of the larger daughter; mode III) or different (mode IV), with no further interaction. In some situations, two bubbles tend to interact closely, exhibiting collision (then possible coalescence) followed by another separation (split), immediately after the breakup (mode V). Under extreme circumstances, the cap may disintegrate into three or more bubbles (mode VI). The latter two modes (V and VI) signify the prevalence of the interactive rise of a group of bubbles ascending side by side in close contact at comparable rise velocities, as has been observed, e.g. as a result of in-line bubbles rising in a liquid-solid fluidized bed (Tsuchiya *et al.* 1989).

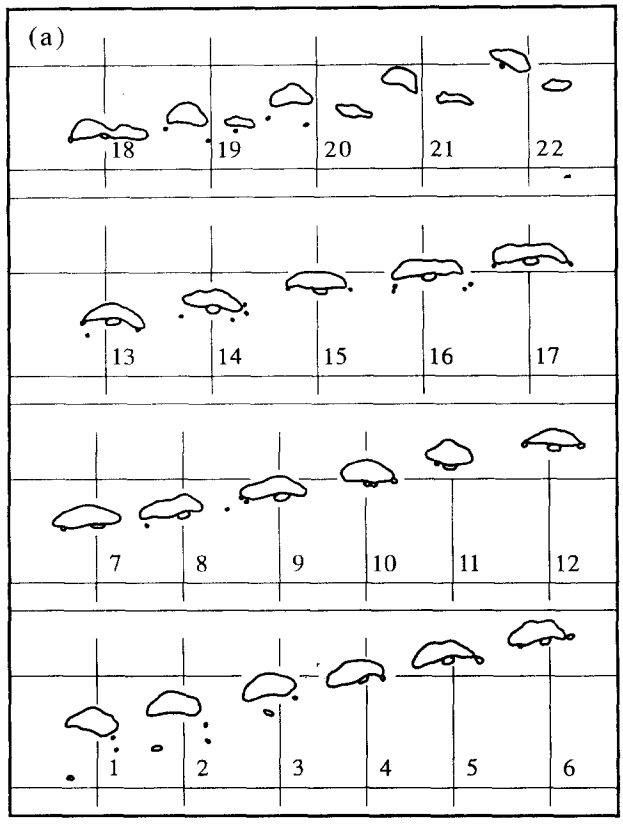

Fig. 2(a). *Caption opposite..*

Shape distortion caused by bubble attachment

Figures 2 and 3 depict two types of cap deformation processes triggered by its close encounter to small bubbles and enhanced by their attachment to the cap base and roof, respectively. The time increment in each step (designated by the number in the figures) is 1/30 s with the initial step being selected arbitrarily. The first type, i.e. the attachment at the base, was observed to often result in indentation on the cap roof at the position right above the attachment point [steps 16–18 in figure 2(a)]. This slight modification of the cap surface could initiate the cap breakup process by the "pinching-off" mechanism described by Tsuchiya *et al.* (1989), as illustrated in a series of sketches in figure 2(a) [note that the small bubble which had triggered the breakup process disappeared (coalesced with the left-side daughter cap) right after the cap breakup event (step 19)]. Based on the present observation of this particular type of cap–bubble interaction, the following hypothesis on a breakup mechanism can be drawn:

> If a large bubble deviates in its shape from the stable cap shape, it will try to restore the deviated portion(s) of the surface to the required shape. This tendency holds even when some small bubbles are attached to its base. The resulting indentation, first at the base then at the roof, induces pinching followed by possible disintegration.

The outcome of this pinching-off mechanism is very sensitive to the location of bubble attachment and the number of attached bubbles. When, for instance, a bubble attaches near the cap edge, it is usually trapped right around the edge (i.e. flow separation point) with some local jitters caused by the vorticity shedding from the edge; the cap together with this "satellite" bubble outlines a required, stable shape with sharp edges [see the right-edge satellite, especially step 18, in figure 2(b)]. Having attached far from the edge, on the other hand, the bubble can trigger the cap split as mentioned above [figure 2(a)]. When multiple bubbles stick to the cap base, they were

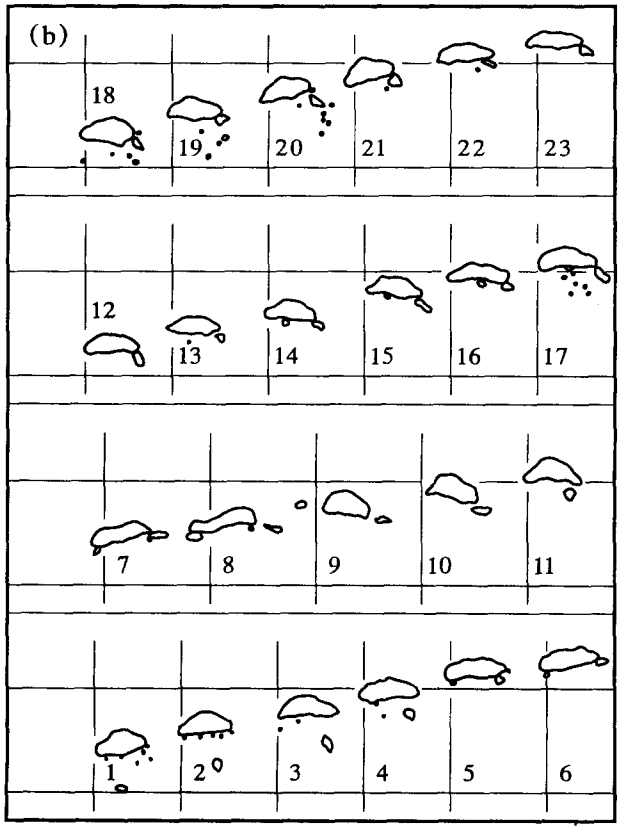

Fig. 2(b)

Figure 2. Sketch of a typical cap deformation process due to bubble attachment at the cap (a) base and (b) edge in water.

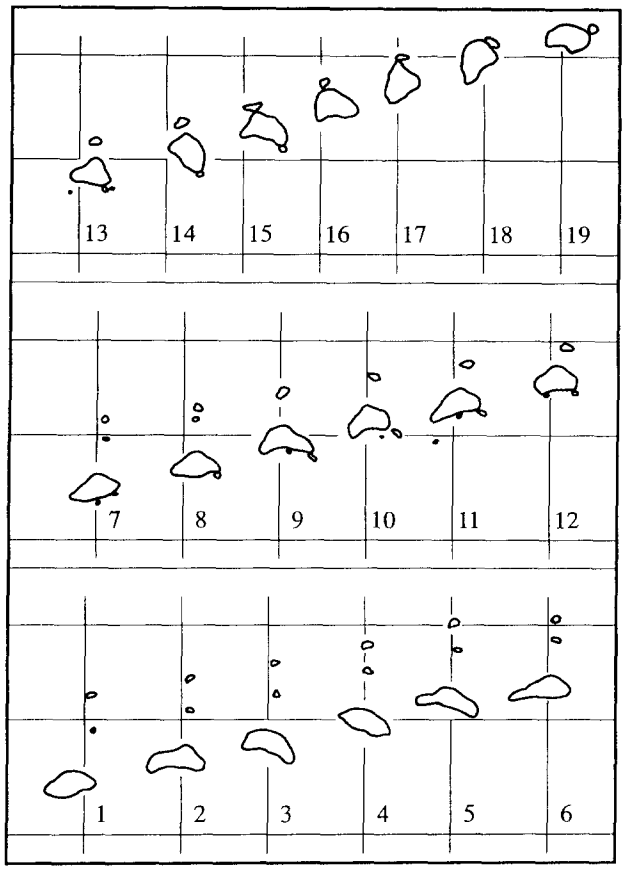

Figure 3. Sketch of a typical cap deformation process due to bubble attachment at the cap roof in water.

observed in this study to usually line up without coalescing along the flat surface; the cap maintains its stable rise with its rear interface partly blocked by those bubbles.

The second type, the attachment at the cap nose in particular, resembles what was observed by Maxworthy (1986) for bubbles in a very narrow (1.8 mm) gap, the so-called Hele–Shaw cell: "When a very small bubble, typically of a diameter of the order of the cell gap width, became attached to the nose of a much larger single bubble, the bubble velocity and ellipticity increased dramatically, by factors of between 2 and 10 depending on the relative sizes of the bubbles. This can be attributed to the subtle change in the boundary conditions at the bubble nose that such a small bubble must induce." A series of sketches in figure 3 illustrate this resemblance. In this particular case, two successive bubbles preceding the cap first coalesed. The cap then started accelerating with appreciable shape distortion (after step 9). By the time the cap contacted the leading bubble at its nose (step 17), the cap shape became prolate, far from its original shape; the cap, however, did not disintegrate, apparently escaping from the influence of the nose bubble (step 19).

Breakup mechanisms

Figure 4 depicts typical patterns of cap disintegration observed in this study. These patterns can be classified into five modes based on the dominating breakup mechanisms: (A) inherent instability of the cap itself; (B) bubble attachment to the cap base, as detailed in figure 2(a); (C) impactive "tackle" of an "intermediate" bubble to the cap base, via the cap wake action; (D) "lifting" of the cap by (usually two) preceding bubbles, apart but horizontally in line, enhanced by the bubble wake action; (E) "suction," into the wake of an intermediate bubble, of part of the nose-peaked (due to bubble attachment; see figure 3) cap. The wake action of both the cap and bubble (of high inertia) stems from its low-pressure characteristics (Fan & Tsuchiya 1990), which can cause a "lift" or "suck" of what is behind. The intermediate bubble could be the result of small bubbles

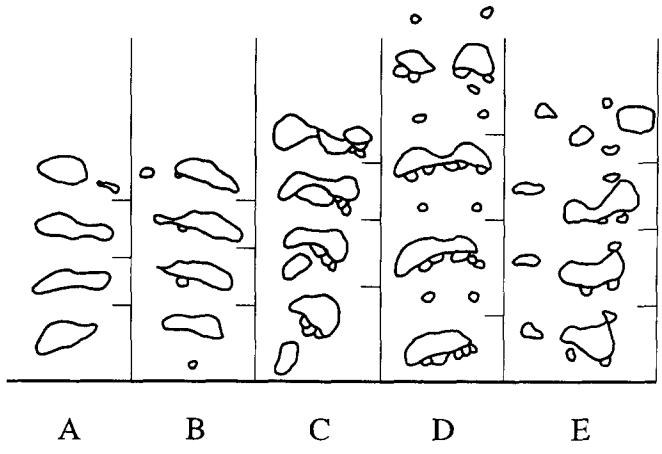

Figure 4. Sketch of typical cap disintegration patterns in water, signifying dominating breakup mechanisms.

coalescence or a segment ruptured from the cap at an earlier stage, observed more frequently at high gas holdups.

Probability of occurrence of specific breakup modes

Out of a large number ($\geqslant 100$) of cap bubbles injected under every condition specified for the bubble swarm (regarding the gas holdup as well as the type of liquid used), each event of the cap–bubble interaction is carefully analyzed and classified into one of the seven modes of interactions (table 3). The probability of occurrence of each mode then is estimated as the fraction of the number of an identical mode of events out of the total number of cap injections. Figure 5(a) shows, for the nitrogen–water system, the plot of cumulative fractions of the representative modes, F, as a function of the swarm gas holdup, ϵ_G; note that relatively resembling modes such as modes III and IV or modes V and VI are combined as a single representative mode. An important

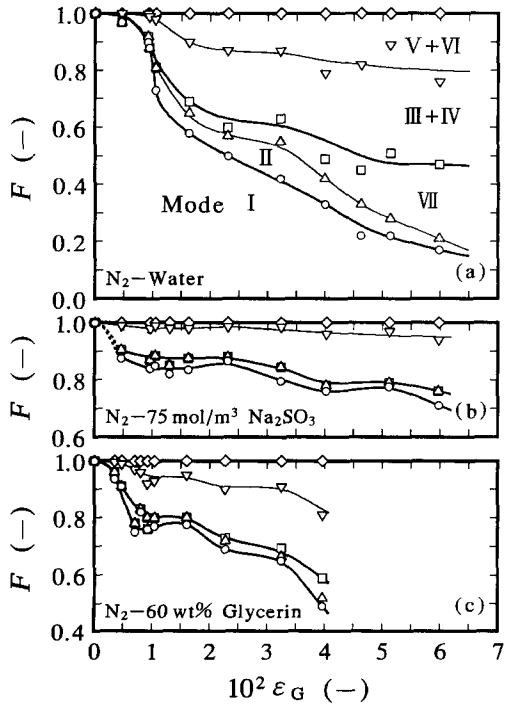

Figure 5. Variation, with swarm gas holdup, in probability of occurrence of various modes of cap–bubble interactions in different liquids.

point to be noted is that there exists a critical gas holdup beyond which the extent of the cap–bubble interactions sharply increases. For tap water, this critical gas holdup occurs at ~ 0.01—the first critical point; the probability involving any interactive patterns (i.e. besides mode I) increases from a negligibly small value to ~ 0.3.

The probability then gradually increases as ϵ_G exceeds 0.015 until ϵ_G reaches in the range of 0.03–0.04—the second critical "region"; above this range the cap is found to possess comparatively high susceptibility to elongation (associated with an increase in the rise velocity); otherwise the cap will break up in over half the occasions. More frequent occurrence of the cap elongation, the second type of cap deformation (see figure 3), at higher ϵ_G can be partially explained in terms of the propagation speed of voidage waves in bubbly flow which tends to decrease, thus encouraging the cap's acceleration toward preceding bubbles, with an increase in the void fraction, i.e. ϵ_G (Lisseter & Fowler 1992).

Figure 5(b) and (c) shows, for the sulfite solution and the glycerin solution, respectively, the corresponding plots for the cumulative fractions. While resembling the overall trend, both liquids exhibit some specific differences from water. First, the first critical point occurs not as sharply as in the case of water: for the sulfite solution, it could not be identified in this study, though confined below $\epsilon_G = 0.005$ if it does exist; for the glycerin solution, the transition occurs in the range 0.003–0.007. Second, cap–bubble interactions are less extensive. The presence of the electrolyte favors high stability of the cap; the cap remains intact as frequently as 80% of the occasions over the entire gas holdup range examined in this study ($\epsilon_G < 0.06$). The dominant interaction patterns are modes III and IV, with cap distortion alone (mode II or VII) being negligible. Increasing liquid viscosity also reduces the degree of interaction, though not as extensively as the electrolyte does. An increase in ϵ_G promotes coalescence of small bubbles, which becomes so appreciable that the bubble swarm can no longer be regarded as homogeneous for ϵ_G exceeding 0.04 with the present glycerin solution. The dominating modes are again III and IV (or V and VI).

Location/height of cap breakup

Figure 6 shows, for tap water, a series of axial probability distributions of the cap–breakup event (covering modes III–VI), f, expressed in terms of histograms, i.e. the discrete probability density

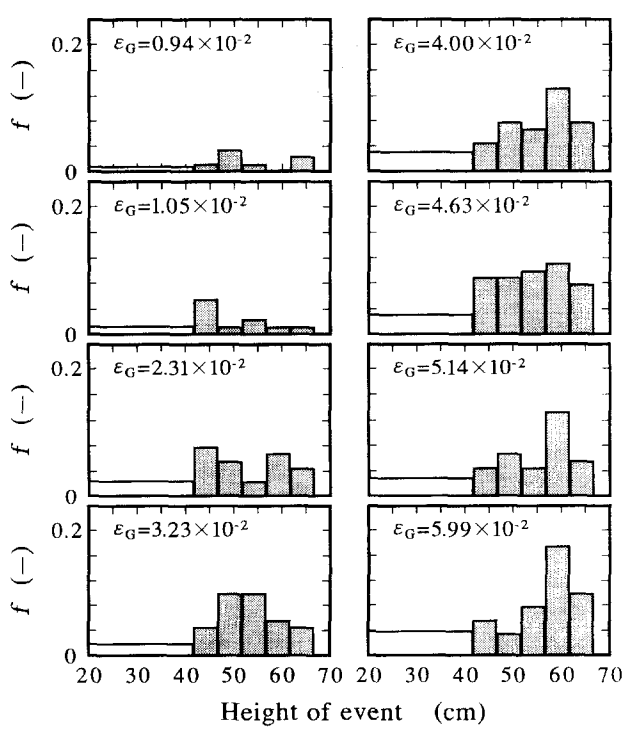

Figure 6. Probability distribution of location of cap-breakup event for different swarm gas holdups in water

or frequency vs the (specific range of) height of the event. The histogram is not normalized in its total area (shaded region), which instead signifies the relative increase in the total probability of cap breakup associated with an increase in ϵ_G. The first large increment in the height (from 0.2 to 0.42 m) is because the occurrence of the event (while visually confirmed) was not recorded in the video system over this zone and its specific location was not determined; the frequency in the histogram was corrected based on the area principle. In the observation zone (from 0.42 to 0.7 m), on the other hand, the height increment was varied to obtain proper (smooth) distributions. As seen in the figure, there appears to be a (global) maximum in the distribution, the axial location of which shows a tendency of shifting from lower values ($\sim$0.4–0.5 m) to higher values ($\sim$0.6 m) as ϵ_G increases from 0.03 to 0.04; with a further increase in ϵ_G, this location remains almost the same while the distribution tends to become sharper. While at present such a trend of the breakup location cannot be explained in a definitive sense, it could be suggested that the rate of change in the voidage speed with void fraction may play some role; note that the time it takes the voidage wave to travel a given vertical distance increases with ϵ_G but becomes almost invariant with ϵ_G with a further increase in ϵ_G (Lisseter & Fowler 1992).

Size ratio after cap split

Figure 7 shows, for tap water, a series of probability distributions of the size ratio of the two daughters (b_2/b_1) resulting from the cap split (modes III and IV), expressed again via histograms. The histogram is prepared in the same manner as that in figure 6 except the ordinate is the absolute number of occurrence, n. When the gas holdup is low (below the first critical value of 0.01), there appears to be no preferable range of size ratio. As ϵ_G exceeds this first critical value but not reaching the second critical range, any size ratios, except for the lowest range, still seem to equally occur with a substantial increase in n. For ϵ_G exceeding this range ($\geqslant$0.04), the distribution tends to be skewed toward the higher ranges of size ratio, i.e. the cap has a tendency to split into two equal-sized daughters (see the right-side column in figure 7).

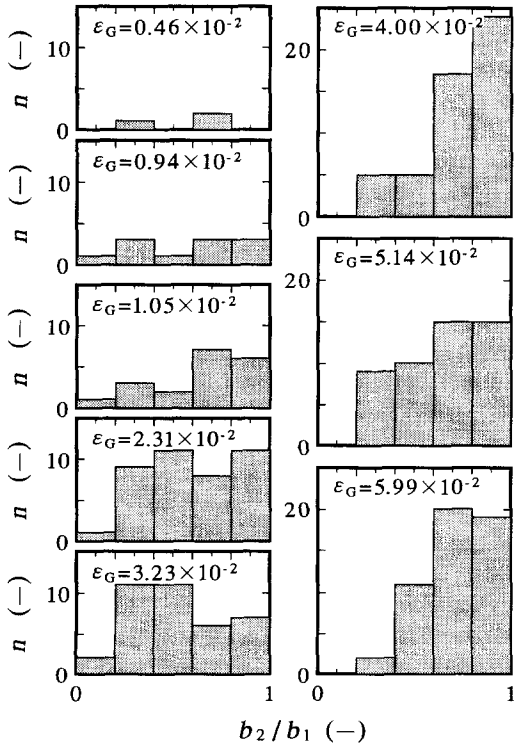

Figure 7. Probability distribution of size ratio of two daughters after cap split for different swarm gas holdups in water.

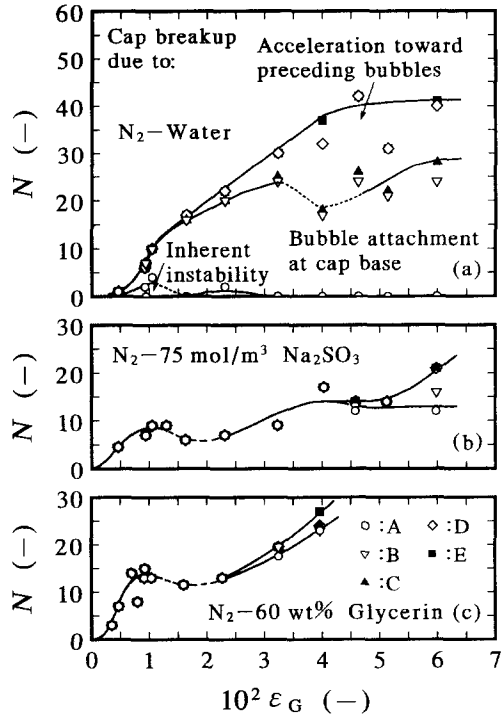

Figure 8. Shift in dominating cap-breakup mechanism with increasing swarm gas holdup in different liquids.

Shift in dominating breakup mechanism

The increase in the swarm gas holdup could cause the dominating breakup mechanism to shift from the inherent instability of the cap itself to the others listed earlier (figure 4). For tap water, as shown in figure 8(a), it is found that the shift takes place first to mechanism B where the bubble attachment at the cap base triggers the ultimate necking or pinching-off (see the marked change in the numbers of distinctive breakup patterns, N, occurring near the first critical point), then to mechanism D, i.e. the lifting of the cap by preceding bubbles under the influence of their wakes (see another change notable within the second critical region). In the figure the dotted portion of the lines signifies the occurrence of the transition. Breakup due to mechanisms C and E is found to be less extensive. The shift in the dominant breakup mechanism from the bubble attachment to the cap acceleration can again be partly explained in terms of the decrease in the voidage wave speed with increasing ϵ_G; the bubble swarm will travel faster at low ϵ_G than high ϵ_G, giving it more chances to approach the cap base at lower ϵ_G but to be caught up with by the cap at high ϵ_G.

For the sulfite and glycerin solutions, however, the relevant shift is only noticeable at higher ϵ_G, as can be seen in figure 8(b) and (c). Over most of the ϵ_G ranges, cap breakup occurs due exclusively to mechanism A—no direct interactions with the surrounding bubbles (claimed to be responsible for the other mechanisms) are apparent, while some indirect influence of the bubbles must have enhanced the breakup frequency; note the general increase in N with ϵ_G in the figures.

Interaction probability and bubble-hole size

The existence of a "hole" of gas holdup in the frontal vicinity of the cap (see introduction) is confirmed visually in this study, and through measurement of light intensity of laser sheets transmitting horizontally across the cap pathway in another study (Ohsaki & Tsuchiya 1994). The size of this bubble hole is found to exhibit a dependency on the gas holdup similar to that exhibited by the probability of the interactive modes, especially regarding the characteristic sharp variation near the first critical holdup (Tsuchiya *et al.* 1995). Figure 9 shows the relationship between the interaction probability, F, and the ratio of the bubble-hole thickness to the cap height, δ/h, for (a) interactive–non-interactive and (b) breakup–non-breakup demarcations; good correlations are obtained between these two parameters. An important implication from this part of the

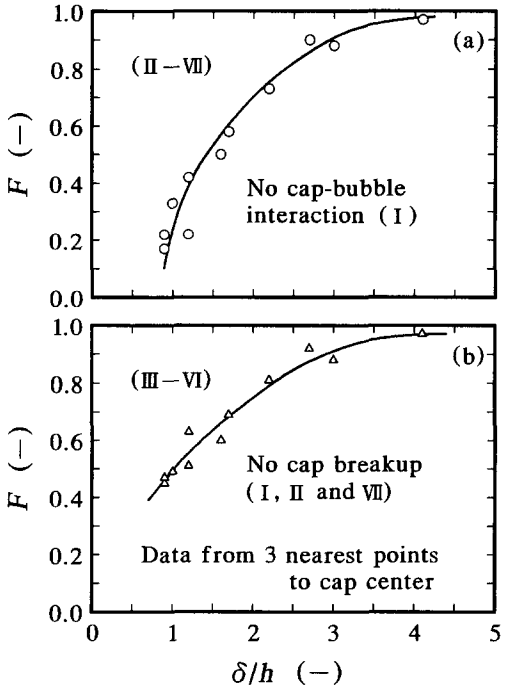

Figure 9. Relationship between interaction probability and bubble-hole thickness for (a) interactive–non-interactive and (b) breakup–non-breakup demarcations in water.

analyses lies in the premise that the probability of occurrence of the cap–bubble interactions (more specifically, the cap disintegration) under the influence of the surrounding swarm bubbles can be predicted based on a less subjective measurement of the bubble-hole size.

CONCLUDING REMARKS

A large cap bubble ascending through a swarm of small bubbles exhibits a variety of shape distortion and breakup patterns, which can fall into one of seven modes identified in the present study. Parallel to this pattern classification, possible mechanism(s) governing a given breakup mode are proposed. The extent of the cap–bubble interactions, generally increasing with the swarm gas holdup, goes through certain transitions; a drastic leap is evident for water at a gas holdup value of ~ 0.01. Adding an electrolyte or raising liquid viscosity tends to reduce this critical holdup value as well as the extent of interactions or to render the transition less drastic. The swarm gas holdup also affects the axial probability distribution of the cap-breakup event, the size ratio of two daughters after the split, or the dominating breakup mechanism. Furthermore, there is a close relationship between the cap stability and the size of the bubble-depleted region immediately above the cap frontal surface.

REFERENCES

Deckwer, W.-D. & Schumpe, A. 1993 Improved tools for bubble column reactor design and scale-up. *Chem. Engng Sci.* **48,** 889–911.

Fan, L.-S. & Tsuchiya, K. 1990 *Bubble Wake Dynamics in Liquids and Liquid–Solid Suspensions.* Butterworth–Heinemann, Stoneham.

Hills, J. H. 1975 The rise of a large bubble through a swarm of smaller ones. *Trans. Instn Chem. Engrs* **53,** 224–233.

Hills, J. H. & Darton, R. C. 1976 The rising velocity of a large bubble in a bubble swarm. *Trans. Instn Chem. Engrs* **54,** 258–264.

Lisseter, P. E. & Fowler, A. C. 1992 Bubbly flow—II. Modelling void fraction waves. *Int. J. Multiphase Flow* **18,** 205–215.

Marks, C. H. 1973 Measurements of the terminal velocity of bubbles rising in a chain. *Trans. ASME, J. Fluid Engng* **95,** 17–22.

Maxworthy, T. 1986 Bubble formation, motion and interaction in a Hele–Shaw cell. *J. Fluid Mech.* **173,** 95–114.

Miyahara, T. & Fan, L.-S. 1992 Properties of a large bubble in a bubble swarm in a three-phase fluidized bed. *J. Chem. Engng Jpn* **25,** 378–382.

Miyahara, T., Tsuchiya, K. & Fan, L.-S. 1991 Effect of turbulent wake on bubble–bubble interaction in a gas–liquid–solid fluidized bed. *Chem. Engng Sci.* **46,** 2368–2373.

Ohsaki, K. & Tsuchiya, K. 1994 Effects of liquid properties on the characteristics of bubble-depleted region above a large bubble. Paper (J103), *Soc. Chem. Engng Japan Autumn Meeting*, Nagoya, 27–29 September.

Tsuchiya, K., Miyahara, T. & Fan, L.-S. 1989 Visualization of bubble–wake interactions for a stream of bubbles in a two-dimensional liquid–solid fluidized bed. *Int. J. Multiphase Flow* **15,** 35–49.

Tsuchiya, K., Ohsaki, K. & Taguchi, K. 1995 The extent of the bubble-depleted region in the frontal vicinity of a large cap bubble rising in a bubble swarm. *Int. J. Multiphase Flow* **21,** 305–313.